Acta Geologica Sinica (English Edition), 2019, 93(6): 1823–1834

High-precision Dating and Geological Significance of Chang 7 Tuff Zircon of the Triassic Yanchang Formation, Ordos Basin in Central China

ZHU Rukai, CUI Jingwei*, DENG Shenghui, LUO Zhong, LU Yuanzheng and QIU Zhen

Research Institute of Petroleum Exploration and Development, Beijing 100083, China

Abstract: The Ordos Basin, as the second largest petroliferous basin of China, contains abundant oil and gas resources, oil shale, and sandstone-type uranium mineral resources. Chang 7 shale is not only the major source rock of the Mesozoic petroliferous system of the Basin, but is also crucial in determining the space-time distribution relationship of the shale section for the effective exploration and development of the Basin's oil and gas resources. To obtain a highly precise age of the shale development section, we collected tuff samples from the top and bottom profile of the Chang 7 Member, Yishi Village, Yaoqu Town, Tongchuan District, on the southern margin of the Ordos Basin and performed high-precision chemical abrasion (CA)–isotope dilution (ID)–thermal ionization mass spectrometry (TIMS) zircon U-Pb dating on the basis of extensive laser ablation inductively coupled plasma mass spectrometry (LA-ICP-MS) zircon U-Pb dating data. Our results show the precise ages of the top and bottom zircon in the Chang 7 shale to be 241.06±0.12 Ma and 241.558±0.093 Ma, respectively. We first obtained Chang 7 age data with Grade 0.1-Ma precision and then determined the age of the shale development in the Chang 7 Member to be the early-Middle Triassic Ladinian. This result is supported by paleontological evidence. The deposition duration of the Chang 7 shale is 0.5Ma with an average deposition rate of the shale section being 5.3 cm/ka. Our research results provide time scale and basic data for further investigation of the basin–mountain coupling relation of the shale section, the sedimentary environment and volcanic ash and organic-matter-rich shale development relation, and the organism break-out and organic-matter enrichment mechanism.

Key words: Ordos Basin, Chang 7 Member, tuff, zircon U-Pb dating

Citation: Zhu et al., 2019. High-precision Dating and Geological Significance of Chang 7 Tuff Zircon of the Triassic Yanchang Formation, Ordos Basin in Central China. Acta Geologica Sinica (English Edition), 93(6): 1823–1834. DOI: 10.1111/1755-6724.14329

1 Introduction

The Ordos Basin, as the second largest petroliferous basin of China, contains rich oil and gas resources, oil shale, and sandstone-type uranium mineral resources. The Changqing Oilfield, currently the largest oil and gas field in China, has achieved a high and stable yield with an oil and gas equivalent of over 50 million tons in the four consecutive years since 2013. As such, it plays a vital role in guaranteeing national energy security, regulating the national energy structure, and promoting economic and social development. The oil exploration target strata of the Triassic Yanchang Formation and the Jurassic crude oil of the Ordos Basin originate mainly from the major source rock of the Chang 7 Member (Zhang et al., 2009; Yang et al., 2013).

In the sedimentary period of the Triassic Yanchang Formation, the Ordos Basin, Chang 7-3 was subjected to rapid lake transgression, which sharply increased the lake depth and range. The lake area in the Chang 7-3 sedimentary period exceeds 10×10^4 km^2, the deep lake water depth reaches 150 m, and the lake water salinity is generally less than 0.1%. As such, it provides a freshwater environment for breeding aquatic organisms and planktons. The temperature difference between the surface and underlying water in the deep lake causes cycles in which this water is suffocated. In these cycles, a large oxygen-deficient area forms in the deep lake, which promotes the development of organic-matter-rich shale. Very thick lake-facies dark-argillaceous sediment has developed such that this high-quality source rock is 20–60 m thick, its distribution range is 5×10^4 km^2, and it mainly consists of dark gray-gray-black carbonaceous mudstone, gray-black mudstone, black shale, and oil shale. Overall, these formations are thin in the west, thick in the east, thin in the north, and thick in the south. The organic matter in the source rock is abundant, and the organic-matter type is good. The average total organic carbon content is 13.75%, and it is dominated by I, II_1 type kerogen, which contains alginite and relatively fewer higher plants (Zhao et al., 1996; Andrew et al., 2007; Zhang et al., 2009).The Chang 7 Member represents the major development period of the Triassic lake transgression in the Ordos Basin and is an indication of the evolution of the Triassic basin deposition. What is its geological background and when did the events causing this Triassic sedimentary evolution occur? What is its relationship with Qinling tectonic coupling? Geologists have long focused on these major scientific questions, but

* Corresponding author. E-mail: cuijingwei@petrochina.com.cn

differences in their understandings have produced different results and further disputes. Using zircon in-situ U-Pb dating with the help of laser ablation inductively coupled plasma mass spectrometry (LA–CIP–MS), Deng et al. (2009) obtained middle-upper and bottom ages for the Chang 7 Member of 221.8±2.0 Ma and 228.2±2.0 Ma, respectively. Zhang et al. (2009) performed dating for the Chang 7 oil shale thin-layered tuff zircon U-Pb and determined two age groups: 242–220 Ma and 220–205 Ma. Zhang et al. (2014) also used LA–CIP–MS in their dating analysis of the Chang 7 tuff zircon and found its age to be 234–236 Ma. Using a sensitive high-resolution ion microprobe (SHRIMP), Wang et al. (2014) determined the age of Chang 7 zircon U-Pb to be 239–241 Ma. Xie (2007) performed dating analysis of the stratum zircon underlying the Chang 8 section tuff in the Tongchuan District and obtained a Chang 8 age of 240.66±0.75 Ma. In summary, Chang 7 zircon dating data from the Ordos Basin has been obtained using secondary ion mass spectrometry (SIMS) and LA-ICP-MS, and the error range of the Chang 7 tuff data is about 2.0 Ma (Deng et al., 2009; Zhang et al., 2009; Wang et al., 2014; Zhang et al., 2014). The difference in the age data for the tuff zircon obtained by various researchers reaches 20 Ma, so it remains uncertain whether the Change 7 Member belongs to Late Triassic or Middle Triassic.

Zircon, with its stable physical and chemical properties, is currently the most important mineral in international isotope chronology research (Sun et al., 2017; Wang et al., 2017; Kang et al., 2018). The zircon dating method is widely applied in the field of earth sciences. Isotopic dilution–thermal ionization mass spectrometry (ID–TIMS) (which requires a Pb background of less than 1 pg in a super-clean laboratory) is deemed to have the highest precision (0.1% RSD), but the Pb and U isotopic spike is technically very difficult and time-consuming. In China, ID–TIMS technology is currently in the exploration stage yet (Landing et al.,2015; Li et al., 2015; Chu et al., 2016; Cox et al., 2018; Wotzlaw et al., 2018). The U-Pb chronological laboratory of the Massachusetts Institute of Technology (MIT) is recognized as having reduced its Pb background to 0.05%. To further investigate the basin–mountain coupling relation in the shale section, the sedimentary environment and the organic-matter-rich shale development relation, and the organism break-out and organic-matter-rich shale development mechanism, for this research, we selected the top and bottom tuffs of the Chang 7 profile in Yishi Village, Yaoqu Town, Tongchuan District on the southern margin of Ordos Basin and we performed zircon chemical abrasion (CA)–ID–TIMS dating at MIT to determine the development age of the Chang 7 shale section, the deposition duration of the shale section, the average deposition rate of the shale section, its time scale, and other basic data.

2 Geological Settings

The Ordos Basin, the second largest sedimentary basin of China, covering an area of 25×10^4 km^2, is a typical superimposed basin, with its marine–marine- and terrigenous-facies cratonic basin in the Paleozoic era and its continental-facies lake basin in Mesozoic era. The basin is located near Lvliang Mountain in the east, Qinling in the south, the Liupan and Helan Mountains in the west, and borders Daqing Mountain in the north (Fig. 1). The Triassic deposition has converted from Carboniferous-Permian marine–continental transitional facies into continental facies and the Yanchang Formation is generally in the greater lake basin period. Its stratum is divided into 10 oil reservoir groups: Change-1–Chang-10, and the Chang 7 oil reservoir group represents the lake basin's greatest lake flooding period, with its sedimentary system dominated by deep-lake–semi-deep lacustrine facies in the south of the Ordos Basin wherein a large area of high-quality source rock is developed (Fig. 1). The lamina of thin-layered tuff in the Chang 7 shale is very developed, with a 182-layer intermediate acidic tuff lamina identifiable in about a 9-m core of the Zheng-8 well in the south of the Basin. This indicates frequent contemporaneous volcanic eruptions during the development of source rock (Zhang et al., 2009). The tuff thickness gradually reduces from the western and southwestern margins of the Basin to the east and northeast, with the tuff most developed in the southern and southwestern margins of the Basin. Contemporaneous eruption and aerial sedimentation are obvious. Chang 7 tuff comprises mainly crystal, vitric, and dual tuffs, and chemical composition analysis of this rock shows its SiO_2 content to be higher (53%), and its pH mainly neutral and acidic (Zhang et al., 2009; Qiu et al., 2009).

3 Samples and Methods

3.1 Samples

We obtained the sampling profile from the Yishi Village, Yaoqu Town, Tongchuan District on the southern margin of the Ordos Basin. Researchers have previously conducted much work on the oil shale resources in this region, thereby providing a basis for stratigraphic division and comparison with this profile. This profile is mainly outcropped with Chang 7 and Chang 8 stratum, in which the shale of the Chang 7 Member is completely outcropped and evenly distributed. The Chang 7 shale section profile of Yishi Village is 26.5 m thick, with our tuff samples taken from the top V13 and bottom V1 of the shale. Figure 2 shows this profile's lithological column and zircon dating sampling position.

3.2 LA–ICPMS zircon U-Pb analysis

We performed LA–ICPMS zircon U-Pb analysis at the University of Arizona. Using the traditional methods of jaw crushing and pulverizing, we extracted zircon grains from whole rock samples, followed by density separation using a Wilfley Table and heavy liquids (methylene iodide). We then separated the resulting heavy mineral fraction using a Frantz LB-1 magnetic barrier separator to isolate the zircons. Then, we incorporated a representative split of the entire zircon yield of each sample into a 1-in epoxy mount along with multiple fragments of each of our four primary zircon standards (FC, SL-F, SL-mix, and R33). We sanded the mounts down ~20 microns, polished them progressively using 9-, 5-, 3-, and 1-micron

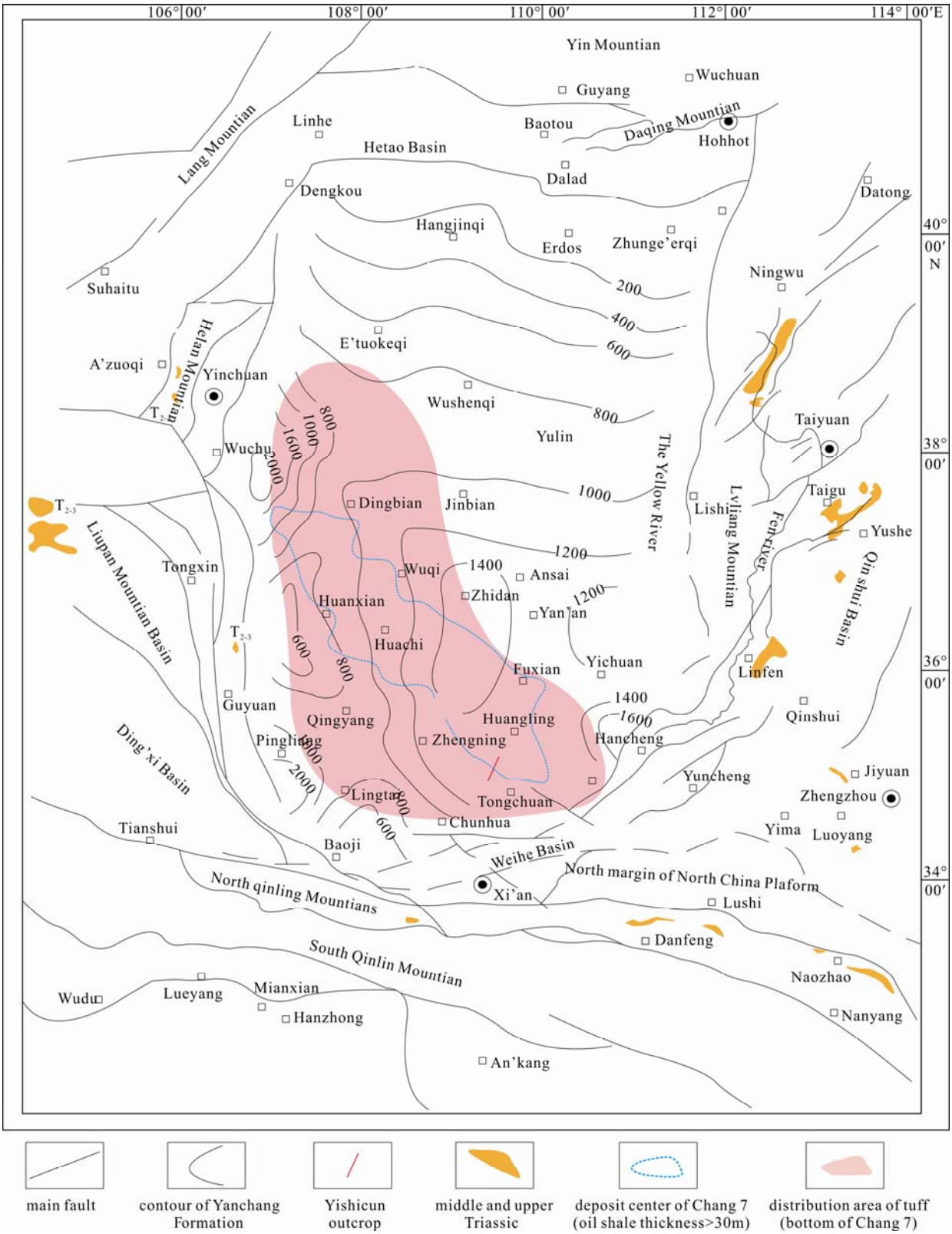

Fig. 1. Sketch of the stratigraphic distribution of Chang 7 Member, Ordos Basin, profile position of Yishi Village and geology on the periphery.

polishing pads, and obtained cathodoluminescence (CL) or backscattered electron (BSE) images using a Hitachi S-3400N scanning electron microscope (SEM) equipped with a Gatan Chroma CL2 detector. Prior to isotopic analysis, we cleaned the mounts in an ultrasound bath of 1% HNO_3 and 1% HCl to remove any residual common

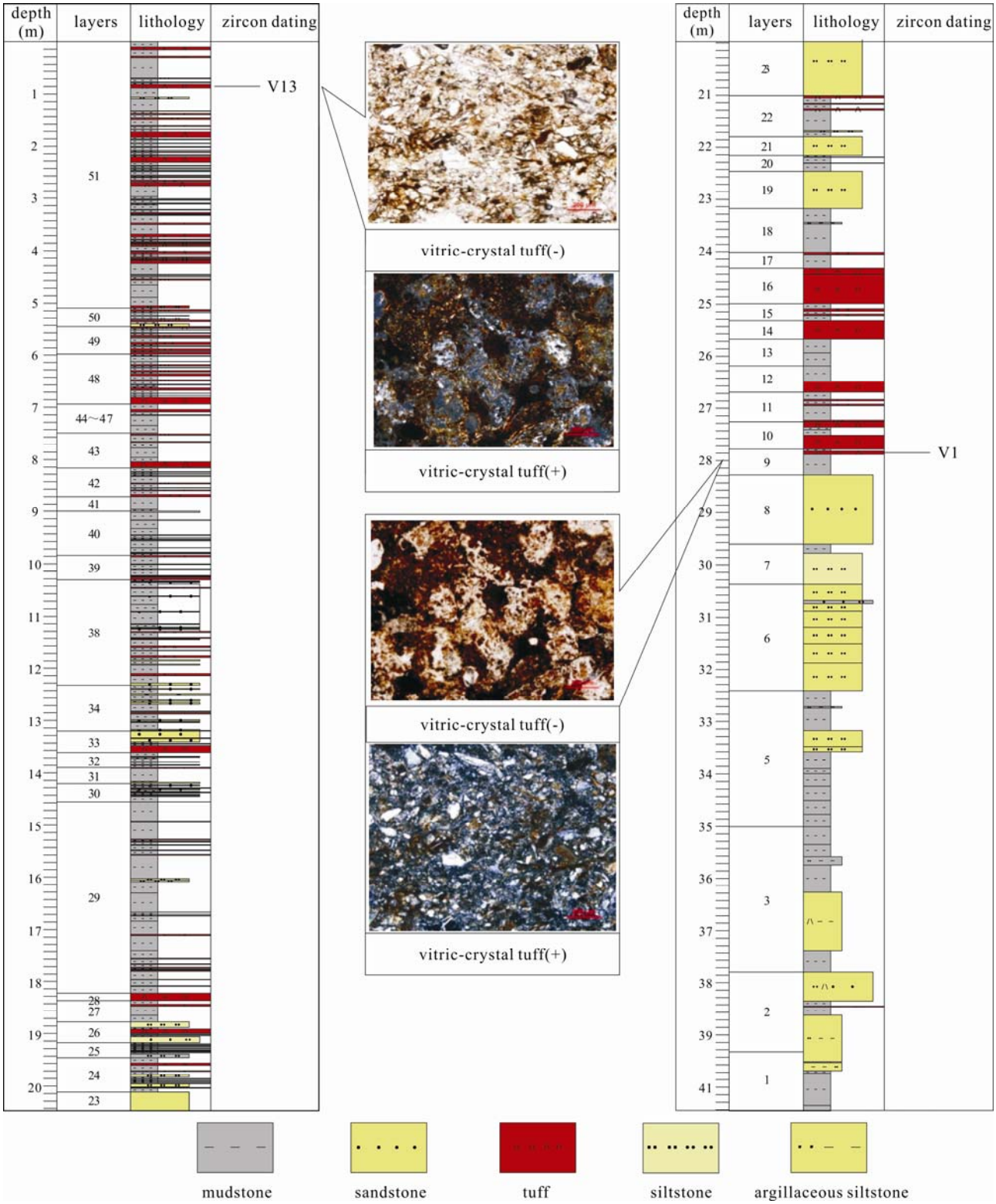

Fig. 2. Profile lithological column in Yishi Village of Ordos Basin and zircon dating tuff sampling point.
0–21 m deep on the left, 21–42 m on the right, photos showing orthogonal light and plane-polarized light of the collected sample.

Pb from the surface of the mount.

We performed our analyses with a laser set at an energy density of ~5 J/cm^2, a repetition rate of 8 Hz, and an ablation time of 10 sec, with ablation pits ~12 microns in depth. The sensitivity of these settings is ~5,000 cps/ppm. Each analysis consists of 5 sec for peaks with the laser off (for backgrounds) and 10 sec with the laser firing (for peak intensities), with a 20 second delay to purge previous sample and save files. Prior to analysis, we obtained images of the grains as a guide for locating analysis pits in

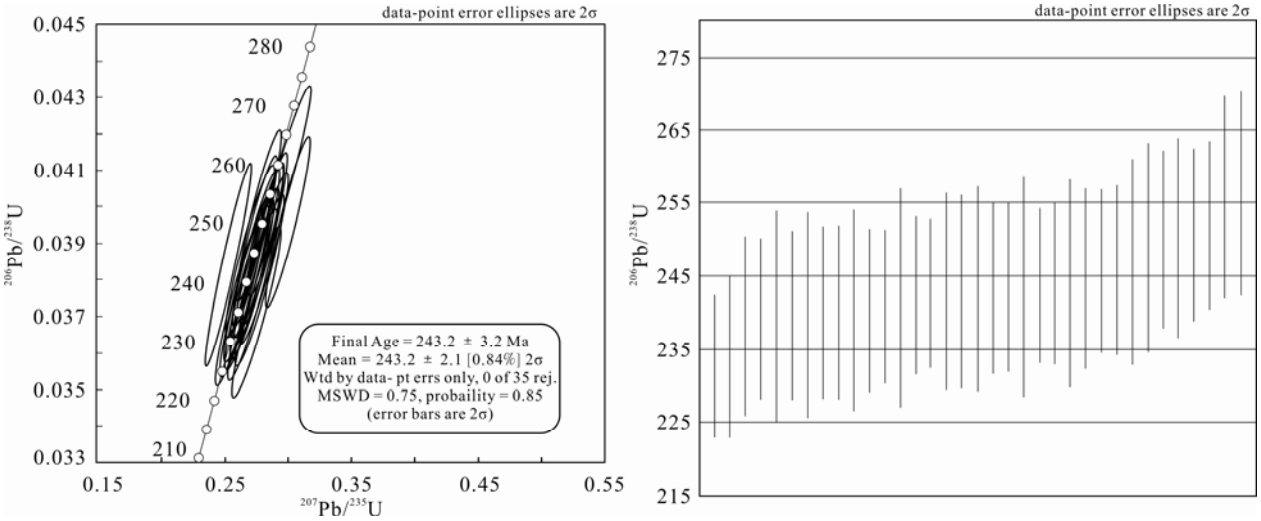

Fig. 3. Result and Error of LA–ICP-MS Zircon Dating of Sample V13 from the Top of the Yishi Village Profile.

Table 1 Igneous V13 U-Pb date summary

Analysis	U (ppm)	$^{206}Pb/^{204}Pb$	U/Th	Isotope ratios $^{206}Pb^*/^{207}Pb^*$	± (%)	$^{207}Pb^*/^{235}U^*$	± (%)	$^{206}Pb^*/^{238}U$	± (%)	error corr.	Apparent ages (Ma) $^{206}Pb^*/^{238}U^*$	± (Ma)	$^{207}Pb^*/^{235}U$	± (Ma)	$^{206}Pb^*/^{207}Pb^*$	± (Ma)	Best age (Ma)	± (Ma)
PetroChina V13 Spot 19	576	8151	2.0	17.6174	1.1	0.2455	3.6	0.0314	3.4	0.95	199.1	6.7	222.9	7.2	482.3	24.9	199.1	6.7
PetroChina V13 Spot 12	1102	17475	2.2	18.3489	1.4	0.2531	3.8	0.0337	3.6	0.93	213.6	7.5	229.1	7.9	391.7	31.5	213.6	7.5
PetroChina V13 Spot 48	665	19050	1.2	18.6524	1.1	0.2715	2.4	0.0367	2.1	0.89	232.5	4.9	243.9	5.2	354.8	24.2	232.5	4.9
PetroChina V13 Spot 37	292	5352	1.4	15.8972	1.7	0.3205	3.0	0.0370	2.4	0.81	233.9	5.6	282.3	7.4	705.0	36.9	233.9	5.6
PetroChina V13 Spot 15	456	6255	1.6	16.3052	0.7	0.3182	2.7	0.0376	2.6	0.96	238.2	6.2	280.5	6.7	650.8	15.7	238.2	6.2
PetroChina V13 Spot 3	656	163767	2.4	19.5362	0.6	0.2668	2.5	0.0378	2.4	0.96	239.2	5.6	240.1	5.2	249.3	14.9	239.2	5.6
PetroChina V13 Spot 49	255	17327	1.8	18.9264	1.0	0.2756	3.2	0.0378	3.1	0.95	239.4	7.2	247.2	7.1	321.8	22.7	239.4	7.2
PetroChina V13 Spot 11	387	1786	1.2	11.7324	1.0	0.4451	2.7	0.0379	2.5	0.92	239.6	5.8	373.8	8.3	1320.9	19.8	239.6	5.8
PetroChina V13 Spot 29	388	18658	1.6	19.8368	0.9	0.2633	3.1	0.0379	3.0	0.95	239.7	7.0	237.3	6.6	214.0	21.7	239.7	7.0
PetroChina V13 Spot 39	207	22431	2.7	19.7599	1.0	0.2646	2.7	0.0379	2.5	0.93	239.9	6.0	238.4	5.8	223.0	22.7	239.9	6.0
PetroChina V13 Spot 21	304	60690	2.0	19.6383	1.0	0.2663	2.7	0.0379	2.5	0.93	240.0	6.0	239.7	5.8	237.3	23.0	240.0	6.0
PetroChina V13 Spot 5	246	16483	1.5	18.9211	0.9	0.2767	3.0	0.0380	2.9	0.96	240.2	6.9	248.0	6.7	322.4	19.4	240.2	6.9
PetroChina V13 Spot 22	362	20628	2.3	18.7988	0.9	0.2785	2.5	0.0380	2.4	0.93	240.3	5.6	249.5	5.6	337.1	20.7	240.3	5.6
PetroChina V13 Spot 23	218	16919	1.2	16.8819	1.5	0.3111	2.6	0.0381	2.2	0.82	241.0	5.1	275.0	6.3	575.8	32.4	241.0	5.1
PetroChina V13 Spot 14	167	21539	1.7	19.2020	1.4	0.2745	3.4	0.0382	3.1	0.91	241.9	7.5	246.3	7.5	288.8	32.3	241.9	7.5
PetroChina V13 Spot 1	188	18530	1.1	19.1132	1.2	0.2763	2.6	0.0383	2.3	0.88	242.3	5.4	247.7	5.7	299.4	28.1	242.3	5.4
PetroChina V13 Spot 20	322	2191	1.4	13.4241	1.8	0.3936	2.8	0.0383	2.2	0.77	242.4	5.1	337.0	8.0	1054.9	35.5	242.4	5.1
PetroChina V13 Spot 18	452	2363	1.4	13.7205	2.4	0.3858	3.7	0.0384	2.8	0.76	242.8	6.7	331.3	10.5	1010.7	48.3	242.8	6.7
PetroChina V13 Spot 9	226	73713	2.1	19.3236	1.0	0.2740	2.9	0.0384	2.8	0.94	242.9	6.6	245.9	6.4	274.4	22.6	242.9	6.6
PetroChina V13 Spot 38	135	3408	0.9	20.9915	0.9	0.2525	3.1	0.0384	2.9	0.95	243.2	7.0	228.6	6.3	81.3	21.6	243.2	7.0
PetroChina V13 Spot 50	209	33677	1.0	18.9913	1.1	0.2793	2.7	0.0385	2.4	0.91	243.4	5.8	250.1	5.9	314.0	25.5	243.4	5.8
PetroChina V13 Spot 24	238	21726	2.2	19.9536	1.1	0.2659	2.7	0.0385	2.4	0.91	243.4	5.8	239.4	5.7	200.4	25.4	243.4	5.8
PetroChina V13 Spot 36	193	13569	1.1	19.1653	1.2	0.2769	3.4	0.0385	3.2	0.93	243.5	7.6	248.2	7.5	293.2	28.1	243.5	7.6
PetroChina V13 Spot 13	160	52568	1.2	19.4976	1.0	0.2724	2.4	0.0385	2.2	0.91	243.6	5.3	244.6	5.3	253.8	23.0	243.6	5.3
PetroChina V13 Spot 43	130	13666	2.2	19.8354	0.9	0.2681	2.5	0.0386	2.3	0.94	224.0	5.6	241.2	5.4	214.2	20.3	244.0	5.6
PetroChina V13 Spot 8	210	27935	2.3	19.6986	1.0	0.2701	3.1	0.0386	3.0	0.95	244.1	7.1	242.8	6.7	230.1	22.8	244.1	7.1
PetroChina V13 Spot 10	246	30282	1.3	19.8260	1.0	0.2690	2.8	0.0387	2.6	0.94	244.6	6.2	241.9	5.9	215.3	22.6	244.6	6.2
PetroChina V13 Spot 4	286	396656	0.6	19.5688	1.0	0.2738	2.5	0.0389	2.3	0.92	245.8	5.6	245.7	5.5	245.4	22.3	245.8	5.6
PetroChina V13 Spot 7	230	49785	1.6	19.3681	0.9	0.2768	2.5	0.0389	2.4	0.93	245.9	5.7	248.1	5.6	269.1	20.6	245.9	5.7
PetroChina V13 Spot 17	287	3900	2.3	15.3824	1.5	0.3500	3.3	0.0390	2.9	0.88	246.9	7.0	304.7	8.6	774.6	32.5	246.9	7.0
PetroChina V13 Spot 26	98	6542	1.4	14.8120	2.0	0.3666	3.5	0.0394	2.9	0.83	249.0	7.1	317.2	9.6	853.6	40.8	249.0	7.1
PetroChina V13 Spot 25	162	94616	2.2	18.2548	1.0	0.2987	2.7	0.0395	2.5	0.93	250.0	6.2	265.4	6.3	403.2	23.0	250.0	6.2
PetroChina V13 Spot 40	185	4126	1.5	16.0299	2.0	0.3403	3.4	0.0396	2.8	0.82	250.1	6.8	297.4	8.8	687.3	41.7	250.1	6.8
PetroChina V13 Spot 35	256	3140	1.8	14.4992	1.9	0.3769	3.1	0.0396	2.4	0.79	250.6	5.9	324.8	8.5	897.8	38.7	250.6	5.9
PetroChina V13 Spot 30	175	15409	1.9	19.7425	1.0	0.2786	2.5	0.0399	2.3	0.92	252.2	5.7	249.5	5.6	225.0	22.1	252.2	5.7
PetroChina V13 Spot 47	245	24528	1.7	17.2585	1.5	0.3234	3.1	0.0405	2.8	0.88	255.8	6.9	284.5	7.8	527.6	33.2	255.8	6.9
PetroChina V13 Spot 27	261	678775	2.9	18.9002	1.1	0.2959	3.0	0.0406	2.8	0.93	256.3	7.0	263.2	6.9	324.9	24.7	265.3	7.0
PetroChina V13 Spot 28	115	10886	1.9	18.3471	1.1	0.3604	2.8	0.0480	2.5	0.92	302.0	7.4	312.5	7.4	391.9	24.8	302.0	7.4

optimal locations and to assist in the interpretation of results. We obtained the images with a Hitachi 3400N SEM and a Gatan CL2 detector system.

Following analysis, we performed data reduction using an in-house Python decoding routine and an Excel spreadsheet (E2agecalc). For the detrital analyses, we used the routines in Isoplot (Ludwig, 2008) to show the ages on Pb*/U concordia and relative age-probability diagrams. The age-probability diagrams show each age and its uncertainty (with respect to measurement error only) as a

normal distribution and then sums all the ages from each sample into a single curve. We then generated composite-age probability plots using an in-house Excel program (see Analysis Tools for link) that normalizes each curve according to the number of constituent analyses, such that each curve contains the same area, and then stacks the probability curves.

For the igneous analyses, we again used Isoplot routines to generate the ages as Pb*/U concordia and weighted mean diagrams (Ludwig, 2008). The weighted mean diagrams show the weighted mean (according to the square of the internal uncertainties), the uncertainty of the weighted mean, the external (systematic) uncertainty that corresponds to the ages used, the final uncertainty of the age (determined by the quadratic addition of the weighted mean and external uncertainties), and the mean-square weighted deviation (MSWD) of the data set.

3.3 ID–TIMS zircon U-Pb analysis

We performed this experiment at the MIT Isotope laboratory. We separated the zircon and other U-bearing silicates from bulk rock samples by the standard crushing, heavy liquid, and magnetic separation techniques, and subsequently handpicked them under a binocular microscope based on their relative clarity and crystal morphology. To overcome the effects of radioactive-decay -induced crystal defects and the associated lead loss, which would result in discordant analyses, we pretreated the zircon grains by the thermal annealing and chemical leaching method or by CA–TIMS (Mattinson, 2005). This method involves heating zircon in a furnace at 900°C for 60 hours. The annealed grains are subsequently loaded into FEP Teflon® microcapsules and leached in concentrated HF at 210°C in high-pressure vessels for 12 hours. The partially dissolved sample is then transferred into Savillex® FEP beakers for rinsing. The leached material is decanted with several milliliters of ultra-pure water and by fluxing successively with 4N HNO_3 and 6N HCl on a hot plate and/or in an ultrasonic bath. After a final rinse with ultra-pure water, zircon grains are loaded back into their microcapsules, spiked with a mixed ^{205}Pb–^{233}U–^{235}U tracer solution and dissolved completely in concentrated HF at 210°C for 48 hours. Essentially, we preferentially remove the high-U parts of the zircon crystals that are associated with Pb-loss, leaving a residue of relatively low U content. After extensive testing, we have concluded that this method is the best possible way for obtaining the most concordant analyses.

4 Results

4.1 Result of LA–ICP-MS zircon U-Pb dating

The zircon yield for the top tuff sample V13 was sufficient for U-Pb laser analysis. These zircons are euhedral, inclusion free, and typically ~50–80 microns in length. We conducted U-Pb analyses with a 20-micron spot diameter, and we based our grain selection and spot placements on CL images that display typical oscillatory zoning (Fig. 3, Table 1). We determined the final age to be 243.2±3.2 Ma, 2-sigma, 0.75 MSWD.

The zircon yield for the bottom tuff sample V1 was also sufficient for U-Pb laser analysis. These zircons are euhedral, inclusion free, and typically ~200–250 microns in length. We conducted U-Pb analyses using a 20-micron spot diameter and our grain selections and spot placements were based on CL images that display typical oscillatory zoning. We determined the final age to be 239.7±2.7 Ma, 2-sigma, 0.7 MSWD (Fig. 4,Table 2).

4.2 Result of ID–TIMS zircon U-Pb dating

We conducted ID–TIMS Zircon U-Pb Dating analyses with six zircons In the V13 volcanic ash samples and four zircons In the V1 volcanic ash samples, respectively. In the V13 volcanic ash samples, we determined the ID–TIMS age of the zircon to be 241.06±0.12 Ma and the Z73 zircon age younger than the others five zircons may affect by the other reasons. (Fig. 5, Table 3). In the V1 volcanic ash samples, we determined the ID–TIMS age of the zircon to be 241.558±0.093 Ma.

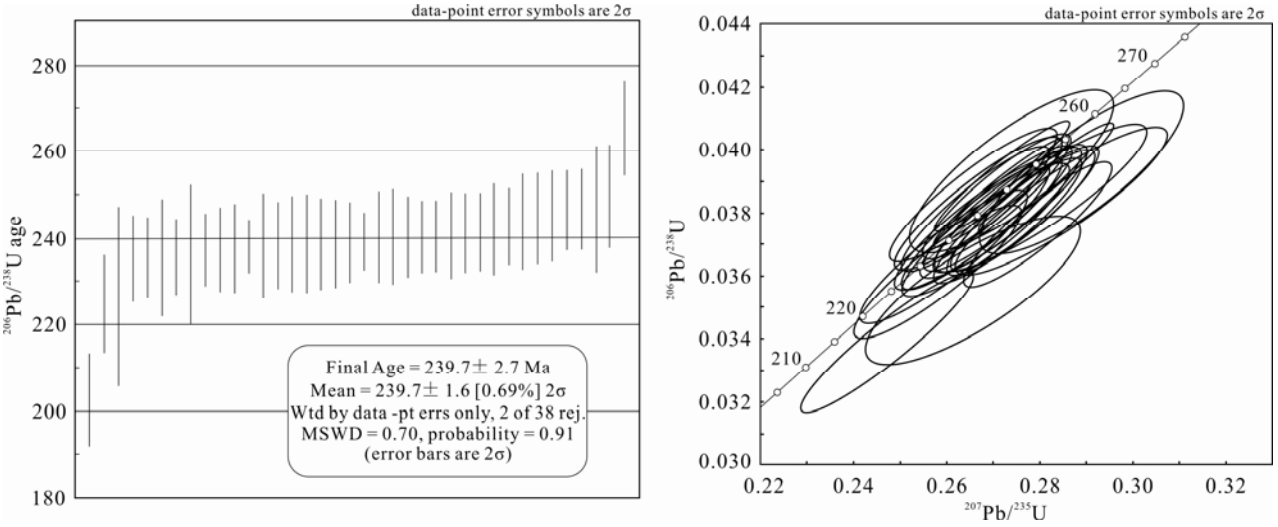

Fig. 4. Result and error of LA–ICP-MS zircon dating of sample V1 from the top of the Yishi Village profile.

5 Discussions

5.1 Age and attribution of Chang 7 shale section

Since 1936, when Professor Pan Zhongxiang determined the Yanchang Formation to have occurred in the Late Triassic Epoch, scholars have found significant differences in the characteristics of the sporopollen assemblage, sedimentary facies, and petrology of the Chang7–Chang1 and Chang10–Chang8 oil reservoir formations (Yong, 1984; Ji et al., 2006; Deng et al., 2009; Chen et al., 2011). Wang et al. (2014) recommended separating the Chang10–Chang8 oil reservoir sections from the Yanchang Formation and calling them the Tongchuan Formation, and attributed the Chang7–Chang1 oil reservoir sections to the range of the Late Triassic Yanchang Formation. We note that the result of U-Pb dating with ICP-MS for this time shows a profile age range of 239.7±2.7–243.2±3.2 Ma, which is basically the same as the previous age determined by the use of SHRIMP (Wang et al., 2014). Although Wang et al. (2014) obtained an age range of 239.7±1.7–241.3±2.4 Ma for the tuff at the bottom of Chang 7, they believed the sedimentary age of tuff to be extremely close to the boundary age of the Ladinian and Carnian Stages, with error consideration, and finally attributed Chang8–Chang10 only to the Middle Triassic Epoch while attributing Chang 7 to the Late Triassic Epoch. Based on a large number of ICP-MS dating results, the age of the tuff zircon at the bottom of the Chang 7 shale section obtained by ID–TIMS is 241.558±0.093 Ma, which is very close to the zircon age of 240.66±0.76 Ma of the Chang 8 section that was experimentally obtained at Washington State University by Xie (2007). According to the latest chronological scale released by the International Commission on Stratigraphy (2016/04), the age of the Chang 7 shale section is attributable to the Ladinian of the Middle Triassic Series (237–242 Ma). The age of the shale top at Yishi Village is 241.06±0.12 Ma. We consider that we have clearly determined the sedimentary age of the Chang 7 shale section of the Yishi Village profile in Yaoqu Town, Tongchuan to be Early Ladinian of the Middle Triassic Epoch.

The Chang 7 section in the Ordos Basin is 100–120 m thick and, if we eliminate event sedimentations such as sedimentary sand bodies of gravity flow and tuff stratum, the average sedimentary thickness is about 100 m. The estimated sedimentary time of the Chang 7 Member is about 1.00 Ma, which accounts for only 10% of the Middle Triassic Epoch (10.1Ma) (Gradstein et al., 2012) (Table 2). The sedimentary time of the 26.5-m shale

Table 2 Igneous sample V1 U-Pb date summary

Analysis	Isotope ratios										Apparent ages (Ma)							
	U (ppm)	206Pb 204Pb	U/Th	206Pb* 207Pb*	± (%)	207Pb* 235U*	± (%)	206Pb* 238U	± (%)	error corr.	206Pb* 238U*	± (Ma)	207Pb* 235U	± (Ma)	206Pb* 207Pb*	± (Ma)	Best age (Ma)	± (Ma)
PetroChina V1 Spot 71	309	8004	0.9	16.2006	1.9	0.2715	3.3	0.0319	2.7	0.83	202.4	5.4	243.9	7.1	664.6	39.8	202.4	5.4
PetroChina V1 Spot 51	127	4656	1.1	18.4452	2.5	0.2652	3.6	0.0355	2.6	0.72	224.8	5.7	238.9	7.6	380.0	55.2	224.8	5.7
PetroChina V1 Spot 55	121	57252	1.8	18.9856	1.1	0.2595	4.8	0.0357	4.6	0.97	226.3	10.3	234.2	10.0	314.7	26.1	226.3	10.3
PetroChina V1 Spot 58	264	46472	2.2	19.4026	1.0	0.2641	2.4	0.0372	2.2	0.91	235.2	5.0	238.0	5.0	265.0	22.0	235.2	5.0
PetroChina V1 Spot 78	237	48397	2.0	18.9298	0.9	0.2709	2.2	0.0372	2.0	0.91	235.4	4.7	243.4	4.8	321.4	21.3	235.4	4.7
PetroChina V1 Spot 57	152	22700	2.2	19.2113	1.2	0.2671	3.1	0.0372	2.9	0.93	235.5	6.8	240.3	6.7	287.7	26.5	235.5	6.8
PetroChina V1 Spot 73	366	31480	4.0	19.4630	0.8	0.2637	2.1	0.0373	1.9	0.92	235.6	4.4	237.6	4.4	257.9	18.5	235.6	4.4
PetroChina V1 Spot 59	191	10436	1.9	19.4304	1.4	0.2646	3.8	0.0375	3.5	0.93	236.0	8.2	238.3	8.1	261.8	31.3	236.0	8.2
PetroChina V1 Spot 53	366	7334501	2.5	19.1045	0.8	0.2706	2.0	0.0375	1.8	0.92	237.2	4.2	243.1	4.3	300.5	18.0	237.2	4.2
PetroChina V1 Spot 83	326	46980	2.4	19.1735	0.8	0.2697	2.2	0.0375	2.1	0.93	237.4	4.8	242.5	4.8	292.2	19.4	237.4	4.8
PetroChina V1 Spot 86	406	9954	1.9	18.5469	0.9	0.2789	2.4	0.0376	2.3	0.93	237.4	5.3	249.8	5.4	367.6	19.8	237.4	5.3
PetroChina V1 Spot 76	341	19766	2.0	19.0221	1.0	0.2727	1.7	0.0376	1.3	0.80	238.1	3.1	244.9	3.6	310.3	22.6	238.1	3.1
PetroChina V1 Spot 72	483	24208	2.5	19.3872	0.9	0.2677	2.8	0.0376	2.6	0.94	238.2	6.1	240.8	5.9	266.9	20.8	238.2	6.1
PetroChina V1 Spot 79	165	8884	1.9	19.6187	1.2	0.2646	2.5	0.0377	2.1	0.87	238.2	5.0	238.3	5.3	239.6	28.1	238.2	5.0
PetroChina V1 Spot 70	104	19941	1.8	18.9784	1.6	0.2739	2.9	0.0377	2.4	0.83	238.5	5.6	245.8	6.2	315.5	35.9	238.5	5.6
PetroChina V1 Spot 82	110	9630	2.5	19.5871	1.5	0.2654	2.9	0.0377	2.5	0.85	238.6	5.8	239.0	6.2	243.3	34.9	238.6	5.8
PetroChina V1 Spot 61	217	12567	2.6	19.2892	1.4	0.2695	2.7	0.0377	2.3	0.84	238.6	5.3	242.3	5.8	278.5	33.0	238.6	5.3
PetroChina V1 Spot 77	530	44715	3.1	19.3713	0.7	0.2685	2.3	0.0377	2.2	0.95	238.7	5.1	241.5	4.9	268.7	15.6	238.7	5.1
PetroChina V1 Spot 81	567	18919	2.6	19.8061	0.8	0.2627	2.1	0.0377	2.0	0.93	238.8	4.6	236.9	4.4	217.6	17.4	238.8	4.6
PetroChina V1 Spot 56	529	16955	3.5	19.6113	0.7	0.2657	1.6	0.0378	1.5	0.91	239.2	3.4	239.3	3.5	240.4	15.9	239.2	3.4
PetroChina V1 Spot 64	131	40421	2.9	19.0925	1.2	0.2741	2.5	0.0380	2.2	0.89	240.1	5.3	246.0	5.5	301.9	26.5	240.1	5.3
PetroChina V1 Spot 69	514	64017	2.9	19.5123	0.8	0.2682	2.5	0.0380	2.3	0.94	240.2	5.5	241.3	5.3	252.1	19.0	240.2	5.5
PetroChina V1 Spot 60	253	11451	2.7	19.4000	0.8	0.2699	2.2	0.0380	2.0	0.92	240.2	4.7	242.6	4.7	265.3	19.5	240.2	4.7
PetroChina V1 Spot 67	589	19447	2.7	18.9771	1.1	0.2759	2.1	0.0380	1.8	0.86	240.3	4.1	247.4	4.5	315.7	24.1	240.3	4.1
PetroChina V1 Spot 62	289	145067	3.0	19.3201	1.0	0.2712	2.0	0.0380	1.8	0.87	240.5	4.1	243.7	4.4	274.8	22.9	240.5	4.1
PetroChina V1 Spot 87	207	18377	2.3	19.1561	1.2	0.2737	2.5	0.0380	2.1	0.87	240.6	5.0	245.6	4.4	294.3	28.2	240.6	5.0
PetroChina V1 Spot 80	220	14036	1.8	19.6669	1.1	0.2672	2.3	0.0381	2.0	0.86	241.1	4.6	240.5	4.8	233.9	26.2	241.1	4.6
PetroChina V1 Spot 54	530	259452	2.8	19.4885	0.8	0.2701	2.1	0.0382	1.9	0.92	241.5	4.5	242.7	4.5	254.9	19.2	241.5	4.5
PetroChina V1 Spot 65	333	9864	2.0	19.8038	1.7	0.2664	2.8	0.0383	2.2	0.80	242.0	5.3	239.8	6.0	217.8	39.4	242.0	5.3
PetroChina V1 Spot 63	240	86747	2.3	19.2563	0.9	0.2747	2.1	0.0384	1.9	0.90	242.7	4.5	246.4	4.6	282.4	21.2	242.7	4.5
PetroChina V1 Spot 85	237	7777	2.0	19.9261	1.1	0.2666	2.6	0.0385	2.3	0.90	243.7	5.5	240.0.	5.5	203.6	25.8	243.7	5.5
PetroChina V1 Spot 66	234	48682	2.9	18.5353	1.5	0.2876	2.7	0.0387	2.2	0.82	244.6	5.2	256.7	6.0	369.0	33.8	244.6	5.2
PetroChina V1 Spot 90	184	50471	3.3	18.7464	1.1	0.2851	2.4	0.0388	2.2	0.90	245.1	5.3	254.7	5.5	343.4	24.5	245.1	5.3
PetroChina V1 Spot 74	246	12724	2.6	19.7587	0.9	0.2718	2.1	0.0390	1.9	0.91	246.3	4.6	244.1	4.5	223.1	19.7	246.3	4.6
PetroChina V1 Spot 84	378	69981	2.8	19.1143	0.8	0.2812	2.1	0.0390	1.9	0.93	246.5	4.7	251.6	4.6	299.3	17.3	246.5	4.7
PetroChina V1 Spot 52	57	72044	1.3	19.7803	2.1	0.2720	3.7	0.0390	3.0	0.82	246.7	7.3	244.3	7.9	220.6	48.0	246.7	7.3
PetroChina V1 Spot 68	88	8891	2.3	18.8054	1.8	0.2895	3.0	0.0395	2.4	0.80	249.6	6.0	258.2	6.9	336.3	40.8	249.6	6.0
PetroChina V1 Spot 88	196	2019	2.4	12.7560	8.9	0.4544	9.1	0.0420	2.1	0.23	265.5	5.4	380.4	29.0	1156.9	176.6	265.5	5.4

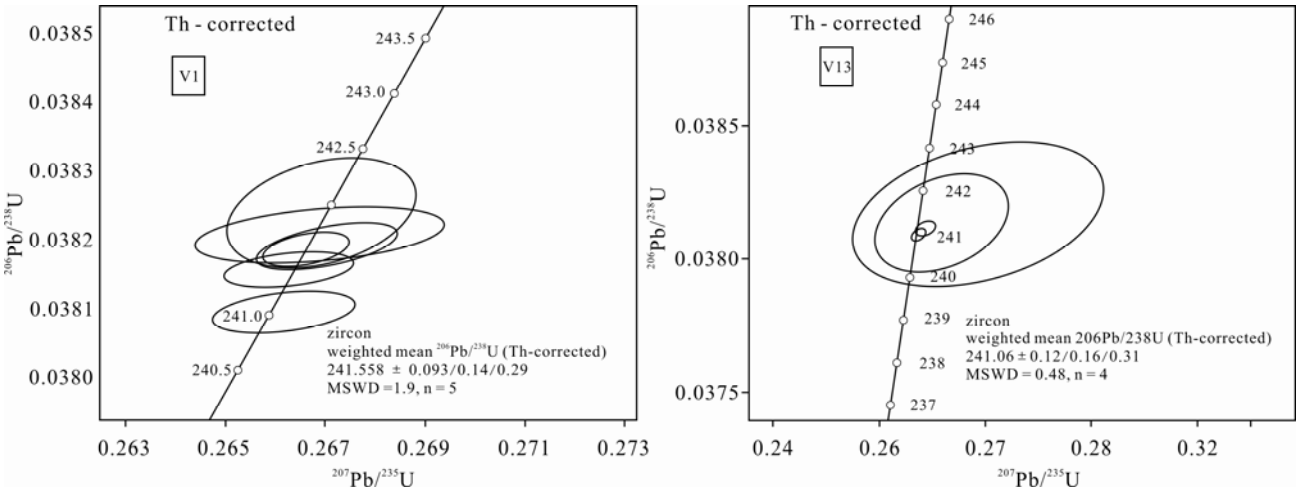

Fig. 5. Results of ID–TIMS dating of two samples for the lithology of the Yishi Village profile in Ordos Basin.

Table 3 CA-ID-TIMS experiment results for zircon samples

Sample	Pb(c) (pg)	Pb* /Pb	Th/U	Ratios								Ages (Ma)						
				$^{206}Pb/^{204}Pb$	$^{208}Pb/^{206}Pb$	$^{206}Pb/^{238}U$	err	$^{207}Pb/^{235}U$	err	$^{206}Pb/^{238}U$	err	$^{207}Pb/^{235}U$	err	$^{207}Pb/^{235}U$	err	$^{207}Pb/^{206}Pb$	err	coef.
(a)	(b)			(c)	(d)	(e)	(2%)	(e)	(2%)	(e)	(2%)		(2%)		(2%)		(2%)	
V1																		
z51	0.6	25.0	1.02	1324.8	0.324	0.038210	(.11)	0.26888	(.92)	0.05106	(.89)	241.73	0.26	241.8	2.0	242	21	0.345
z55	0.3	44.4	0.46	2689.8	0.145	0.038191	(.09)	0.26911	(.50)	0.05113	(.46)	241.61	0.22	242.0	1.1	246	11	0.411
z57	0.3	44.7	0.54	2644.4	0.171	0.038159	(.07)	0.26830	(.48)	0.05102	(.46)	241.41	0.16	241.3	1.0	241	11	0.393
z58	0.5	31.7	0.49	1907.4	0.156	0.038240	(.21)	0.26892	(.71)	0.05103	(.66)	241.91	0.50	241.8	1.5	241	15	0.364
z73	0.3	43.5	0.36	2703.5	0.114	0.038098	(.08)	0.26819	(.53)	0.05108	(.50)	241.03	0.19	241.2	1.1	243	12	0.397
z78	0.4	60.6	0.42	3703.1	0.132	0.038186	(.07)	0.26858	(.35)	0.05103	(.33)	241.58	0.17	241.55	0.75	241.3	7.6	0.377
V13																		
z21	0.3	46.9	0.65	2704.6	0.204	0.038093	(.07)	0.26838	(.46)	0.05112	(.44)	241.00	0.16	241.40	0.99	245	10	0.356
z23	0.2	36.5	0.98	1941.4	0.310	0.038113	(.07)	0.26959	(.63)	0.05132	(.61)	241.13	0.18	242.4	1.4	254	14	0.331
z48	0.4	4.7	0.77	279.3	0.244	0.038133	(.49)	0.27284	(4.56)	0.05191	(4.42)	241.3	1.2	245.0	9.9	281	101	0.325
z49	0.9	2.3	0.61	150.5	0.193	0.038165	(.73)	0.27941	(8.44)	0.05312	(8.23)	241.5	1.7	250	19	333	187	0.330

Note: (a) Thermally annealed and pretreated single zircon, (b) Total common Pb in analyses, (c) Measured ratio corrected for spike and fractionation only, (d) Radiogenic Pb, (e) Corrected for fractionation, spike, and blank. Also corrected for initial Th/U disequilibrium using radiogenic ^{208}Pb and Th/U[magma] = 2.8

section of the Yishi Village profile in Yaoqu Town is about 0.5 Ma, with a sedimentation rate of 5.3 cm/ka, which is much lower than the 24-cm/ka rate of the coeval Triassic lacustrine facies (Oslen, 1986). This low sedimentation rate may be one of the factors accounting for the organic-matter enrichment in the Chang 7 Member. Considering that the dating results of other oil reservoir formations have yet to be obtained and that only the Chang 7 shale section is attributed to the early-Middle Triassic Epoch, we further discuss the attribution of other oil reservoir formations of the Yanchang Formation here with reference to paleontological evidence.

In fact, there are abundant paleontological fossils in the Yanchang Formation and their study began over a century ago with the study of flora by Krasser (1900). Its flora was then compared with Lunzer-Keuper of Austria and Basler-Keuper of Switzerland based on phytoliths and its age was determined to be of the Late Triassic Epoch. However, in comparison with the Keuper flora in Europe, systematic studies later determined that the phytolith produced in the Yanchang Formation could be divided between two floras, with the lower produced in strata below the Chang 7 stratum with an age of the Middle Triassic Epoch and the upper produced in the strata above the Chang 7 stratum with an age of the Late Triassic Epoch. The study results for sporopollen are basically consistent with those of plant macrofossils and results published in recent years have further supported this conclusion (Wang et al., 2003; Jiang et al., 2006; Ji et al., 2006; Deng et al., 2009). Paleontological studies of plants and sporopollen have been conducted in the Yanchang Formation, with typical early-Middle Triassic lycopod fossils found in the Chang 8 and Chang 7 strata, including Pleuromeia and Annalepis. Globally and thus far, these two genera have been found to belong to the Middle and Lower Triassic Series (Fliche, 1910; Retallack, 1975; Wang et al., 1978; Wang et al., 1982; Kelber, 1990; Mader, 1990; Grauvogel-Stamm et al., 1983; Grauvogel-Stamm et al., 2001; Yu et al., 2008; Yu et al., 2010), which indicates that the age of the Chang 7 stratum and the strata below it will not be earlier than the Middle Triassic Epoch. Studies of several profiles in the region indicate that the evolution of the palynoflora can be divided into two stages. The Chang 8 stratum and the strata below are very rich in sporopollen fossils, similar to the overall appearance of the Middle Triassic Zhifang Formation. Chang 7 is poor in fossils, but the diversity of cyclosporine is obviously increased, which indicates that the appearance of flora had begun to change. Chang 6 stratum and the strata above are rich in sporopollen, and appear to belong to the Late Triassic Epoch. Most of the

Table 4 Division scheme of Chang 7 stratum of Yanchang Formation in Ordos Basin

System	Series	International stage[a]	Age (Ma)[a]	Formation[b]	Member[b]	Oil Reservoir Formation[b]	Thickness (m)[b]	(ID–TIMS) Dating	This paper
Triassic System	Upper Triassic	Rhaetian	201.3 209.5	Yanchang Formation	T_3y^5	Chang 1	0–240		Rhaetian
		Norian	209.5 228.4		T_3y^4	Chang 2	120–150		Norian
						Chang 3	90–110		
		Carnian	228.4 237.0		T_3y^3	Chang 4 and Chang 5	80–90		Carnian Ladinian
						Chang 6	110–130		
						Chang 7	100–120	241.558 ± 0.093Ma	
	Middle Triassic	Ladinian	237.0 241.5	Tongchuan Formation	T_3y^2	Chang 8– Chang 9	75–90 to 80–110		Anisian
					T_3y^1	Chang 10	210–350		
		Anisian	241.5 247.1	Zhifang Formation					
	Lower Triassic	Olenekian	247.1	Heshanggou Formation					Olenekian
		Induan	252.2	Liujiagou Formation					Induan

Note: (a) international stage and absolute age are based on the work of Gradstein, 2012; (b) formation and thickness are based on Deng Xiuqin et al., 2013 and Wang et al. 2014.

study results for lacustrine organisms in the strata below the Chang 7 stratum, including bivalves, conchostracans, and ostracods, support the view that it belongs to the Middle Triassic Epoch. The ichthyolite Hybodus youngi found in the Chang 7 oil shale also has the characteristics of the late Middle Triassic Epoch. As such, the paleontological fossil evidences support the zircon age data result. That is to say, we attribute the Chang 7 stratum of the Yanchang Formation and strata below it to the Middle Triassic, and the strata above Chang 6 to the Upper Late Triassic.

5.2 Possible resources of tuff in Chang 7 Member

With the area of tuff in the Chang 7 Member being greater than 3×10^4 km^2 and distributed in the Basin's west and southwest, it has received much research attention with respect to stratigraphic division, determination of critical incident time, formation mechanism of organic-matter-enriched shale, and the relationship between the Ordos Basin and peripheral orogenesis. As such, as reference, it is important to study the genesis of the lake basin in the Ordos Basin, the supply of the provenance system, and the response to the tectonic sedimentation (Zhou et al., 1994; Deng et al., 2008; Zhang et al., 2009; Xie, 2007). The main provenances of the Yanchang Formation in the Ordos Basin derive from the south, southwest, and west. Also, the provenances at different periods were supplied in different ways (Deng et al., 2008; Xie, 2007). Although many studies have shown that the formation and evolution of the Triassic lacustrine basin in the Ordos Basin are associated with the collision and splicing of the North China Craton and the Yangtze Continental Block, as well as the Qinling orogenesis, recent studies have been unable to determine the source of the Chang 7 tuff. Based on its age (234–236 Ma), Zhang et al. (2014) speculated that Chang 7 may be associated with the closing of the Paleozoic Ocean Basin in the Mianlue Belt and the consequent subduction of the continental basement under the South Qinling Microplate. Zhang et al. (2009) believe the crater to have resulted from the Qinling Orogenic Belt adjacent to the south of the lake basin. Based on the distribution feature of the Chang 7 tuff, Wang et al. (2014) assumed that the crater may be located in the Qinling–Qilian Orogenic Belt situated on the southwest edge of the Basin. Based on clastic zircon dating results, Xie (2007) consider that Chang 8 to Chang 4+5 sedimentary parent sources from the Tongchuan Region in the south and southwest of the Basin are Qilian–Qaidam terranes, so the Qinling Orogenic Belt had made a few contributions. The authors determined the U-Pb age of the Chang 7 tuff to be the Middle Triassic. On this basis, the magmatic-rock active region of the corresponding age may be the potential tuff source region.

Zhang et al. (2013) summarized 257 age data and found that the zircon TIMS U-Pb age of the Xiangride granitic mass in the south of Xiangride Town situated on the south edge of Qaidam Basin in the south of Qilianshan Tectonic Zone is between 251 Ma and 232 Ma, with an average of 242 Ma; the SHRIMP U-Pb age is 242±2 Ma; and the zircon TIMS U-Pb age of the Chahannuo rock mass is between 251±5 Ma and 232±5 Ma (Yin et al., 2013; Liu et al., 2004; Chen et al., 2007). Moreover, the discovery of a synchronous granite mass indicates that the above two regions are situated in the volcanic areas in the Middle Triassic, which may be one of the potential source regions of the Chang 7 tuff (Fig. 6).

Nevertheless, based on isotopic dating statistics for granite, metamorphic rock, and the polymetallic deposit in the Qinling Orogenic Belt, the age with most abundant activities has been found to be 210–224 Ma, followed by 198–206 Ma. Also, a few of these ages are distributed between 230 Ma and 238 Ma (Deng et al., 2009). In

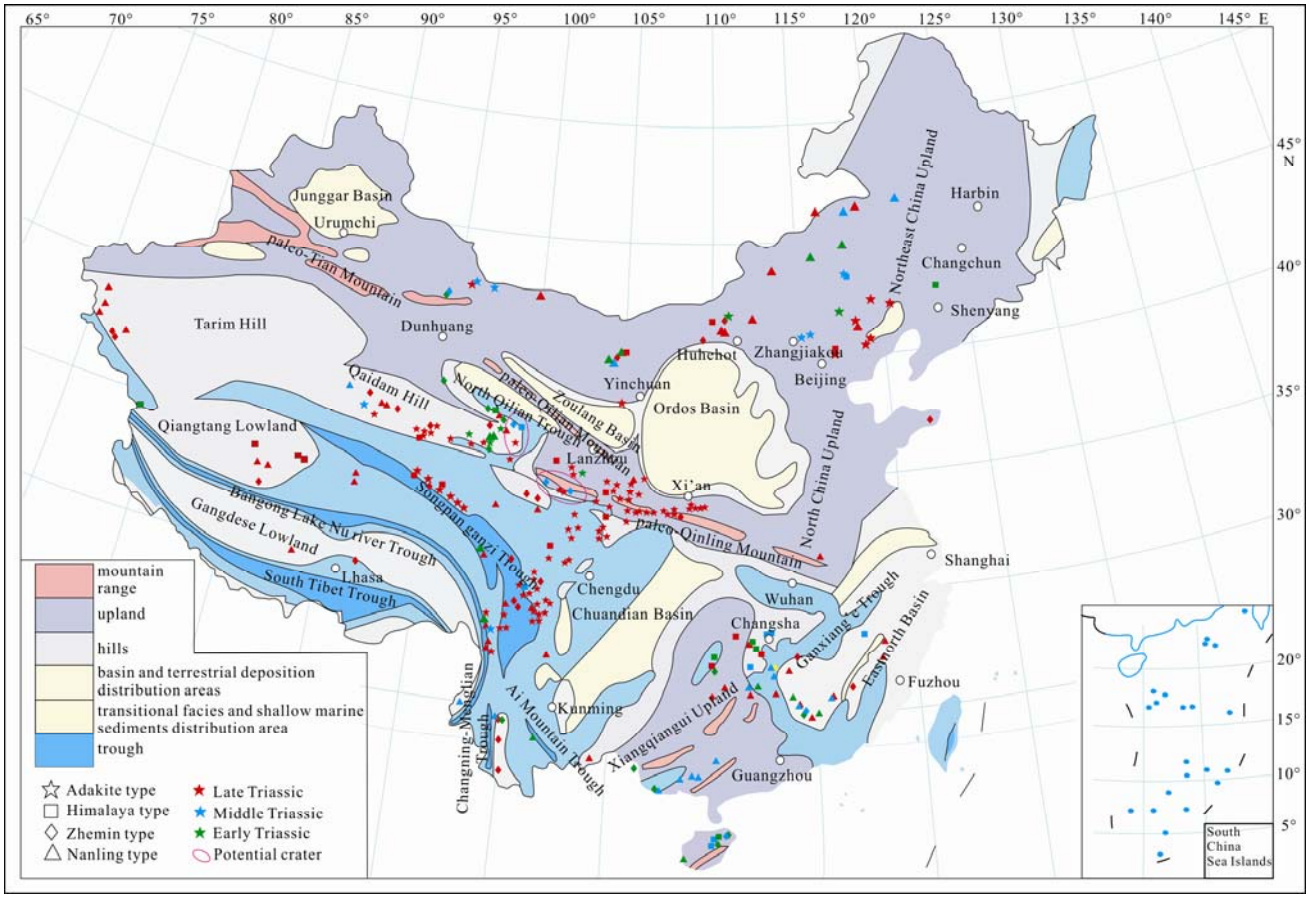

Fig. 6. Triassic paleogeographical map, granite distribution region and potential crater.
Topographic map and granite distribution modified by Zhang, Q. et al., 2013; China basemap after China National Bureau of Surveying and Mapping Geographical Information.

addition, these rocks are mainly distributed in the north of the Mianlue stylolite, west of East Qinling, and in the West Qinling Region. Recently, the zircon U-Pb ages in West Qinling, Miba, Guangtou Mountain and East Jiangkou in the adjacent region were determined to be distributed in the range 206–220 Ma. The zircon age of Rilongguan granite is 195±6 Ma and 181±4 Ma. The age of Barkam granite is 188±2 Ma and 153±3 Ma (Rodge et al., 2004). Granite in the Qinling Region mainly developed in the Late Triassic, but that in the Middle Triassic is only sporadically distributed in the West Qinling Orogenic Belt (Fig. 6). The U-Pb dating of adakitic granites from Yeliguan and Xiahe in West Qinling indicates ages of 245±6 Ma and 238±4 Ma, Meiwu rock mass in the corporation region ranges from 245–242 Ma, and the ages of the gabbro diorite and hornblende andesite are 243.8±1.0Ma and 242.1±1.2Ma, respectively, which is close to the experimental result (Jin et al., 2005; Guo et al., 2011; Luo et al., 2012). Moreover, the U-Pb weighted average age of the granodiorite in the Ayi Mountain, Xiahe in the connection with the Qinling and Qilian Orogenic Belts in the north section in the west of the West Qinling Orogenic Belt is 241.6±4 Ma (MSWD = 0.44), which is closest to the dating result. Therefore, this confirms that the above regions are volcanic in the Middle Triassic, and may be a crater (Fig. 6).

Based on the age of the Triassic granite in the periphery of the Ordos Basin, we speculate that the two regions with stronger volcanic activities in the same period may be the source of tuff (namely, the adakitic granite from Yeliguan and Xiahe in West Qinling and the Xiangride granitic mass in the south of Xiangride Town situated on the southern margin of Qaidam Basin). In accordance with the precise age of the Chang 7 tuff in the profile of Yishi Village, we consider it unlikely that the volcanic ash is from the Qinling Orogenic Belt in the south, but rather that it is likely from Yeliguan and Xiahe in the south of Gansu in the west of the Basin or the Xiangride region in the east of Qinghai.

6 Conclusions

In this study, we obtained the age of the Chang 7 Member profile with a precision of 0.1 Ma, first by performing tuff zircon U-Pb dating at the top and bottom of the sectional Chang 7 tuff in Yishi Village, Yaoqu Town, Tongchuan Region in the southern margin of the Ordos Basin.

We determined the precise ages of the zircons at the top and bottom of the Chang 7 shale to be 241.06±0.12 Ma and 241.558±0.093 Ma, respectively. The Chang 7 shale developed in the early Ladinian Stage of the Middle

Triassic and was continuously deposited for 50 Ma at an average sedimentary speed of 5.3 cm/ka.

On this basis, we determined that its crater may located in the adakite granite in Yeliguan and Xiahe in West Qinling or in the Xiangride granitic mass in the south of Xiangride Town. Furthermore, with respect to the Qilian Orogenic Belt, the coupling relation between the Ordos Basin and its peripheral orogenic belt established the basin –range coupling pattern "Qinling Orogenic Belt–Qilian Mountain Orogenic Belt–Ordos Basin."

Acknowledgements

This study was supported by the National Basic Research Program of China (973 Program) granted No. 2014CB239001. We are deeply grateful for Pecha, Mark E of Department of Geosciences, University of Arizona for assistance on the LA–ICPMS zircon U-Pb analysis and helpful comments. We also thank Dr Jahandar Ramezani of Massachusetts Institute of Technology for assistance on the CA-ID-TIMS zircon U-Pb analysis.

Manuscript received Aug. 1, 2018
accepted Dec. 20, 2018
associate EIC HAO Ziguo
edited by LIU Lian

References

Andrew, D.H., Bradley D.R., and Moldowan, J.M., 2007. Organic geochemistry of oil and source rock strata of the Ordos Basin, north-central China. AAPG Bulletin, 91: 1273–1293.

Chen, N.S., Wang, X.Y., and Zhang, H.F., 2007. Geochemistry and Nd-Sr-Pb isotopic compositions of Granitoids from Qaidam and Oulongbuluke Micro-Blocks, NW China: constraints on basement nature and tectonic affinity. Earth science-Journal of China University of Geosciences, 32(1): 7–21 (in Chinese with English abstract).

Chen, A.Q., Chen, H.D., and Hou, M.C., 2011. The middle-late Triassic event sediments in Ordos basin: indicators for episode I of the Indosinian Movement. Acta Geologica Sinica, 85(10): 1681–1690 (in Chinese with English abstract).

Cox, G.M., Isakson, V., Hoffman, P.F., Gernon, T.M., Schmitz, M.D., Shahin, S., and Nordsvan, A., 2018. South Australian U -Pb zircon (CA-ID-TIMS) age supports globally synchronous Sturtian deglaciation. Precambrian Research, 315: 257–263.

Chu, Z.Y., Xu, J.J., and Chen, Z., 2016. Ultra-low blank analytical procedure for high precision CA-ID-TIMS U-Pb dating of single grain zircons. Chinese Science Bulletin. 2016 (10): 1121–1129 (in Chinese with English abstract).

Deng, X.Q., Li, W.H., and Liu, X.S., 2009. Discussion on the stratigraphic boundary between middle Triassic and Upper Triassic. Acta Geologica Sinica, 83(8): 1089–1096 (in Chinese with English abstract).

Deng, X.Q., Lin, X.F., and Liu, X.Y., 2008. Discussion on relationship between sedimentary evolution of Triassic Yanchang Formation and the early Indosinian movement in Ordos basin. Journal of palaeogeography, 10(2): 159–166 (in Chinese with English abstract).

Fliche, P., 1910. Flore fossil du Trias en Lorrain et France-Comté avec des Considérations finales par MR Zeiller. Bull de la Société des sciences de Nancy, 2(3): 222–286.

Guo, X.Q., Yan, Z., and Wang, Z.Q., 2011. Geological characteristics and associated magmatic ages of the Xiekengskarn-typeCu-Au depositin the West Qinling terrane. Acta Petrologica Sinica, 27(12): 3811–3822 (in Chinese with English abstract).

Grauvogel-Stamm, L., and Duringer, P., 1983. Annalepis zeilleri Fliche 1910 emend., un organe reproducteur de Lycophyte de la Lettenkohle de l'Est de la France: Morphologie, spores in situ et paléoécologie. Geologische Rundschau, 72(1): 23–51.

Grauvogel-Stamm, L., and Lugardon, B., 2001. The Triassic lycopsids Pleuromeia and Annalepis: relationships, evolution, and origin. American Fern Journal, 91(3): 115–149.

Gradstein, F.M., Ogg, J.G., and Schmitz, M.D., Ogg, G.M. 2012. The Geologic Time Scale. Holland: Elsevier, 716–718.

Ji, L.M., Wu, T., and Li, L.T., 2006. Paleoclimatic characteristics during sedimentary period of main source rock of Yanchang Formation (Triassic) in eastern Gansu. Acta Sedimentological Sinica, 24(3): 426–431 (in Chinese with English abstract).

Jiang, D.X., Wang, Y.D., and Wei, J., 2006. Palynoflora and its environmental significance of the Late Triassic in Tongchuan, Shaanxi province. Journal of plaeogeography, 8(1): 23–33 (in Chinese with English abstract).

Jin, W.J., Zhang, Q., and He, D.F., 2005. SHRIMP dating of adakites in western Qinling and their implications. Acta petrologica Sinica, 21(3): 959–966 (in Chinese with English abstract).

Kelber, K.P., 1990. Die versunkene Pflanzenwelt aus den Deltasümpfen Mainfrankens vor 230 Millionen Jahren: Makrofloren aus dem Germanischen Unterkeuper. Würzburg: Freunde der Würzburger Geowissenschaften, 1: 1–67.

Krasser, F., 1900. Die von W.A. Obrutschew in China und Centralasien 1893-1894 gesammelten fossilen Pflanzen. Debkschr. K. Akad. Wiss. Wien, Math-Nat. Cl., 70: 139–154.

Kang, Y., Chen, G., Xia, X.Y., Ren, S.F, Zhang, W.G., and Shi, P.P., 2018. Detrital zircon U-Pb geochronology and its geological implication of the Nancaode and Zhuanghegou Formation in the Southern Margin Ordos basin. Acta Geologica Sinica, 92(9): 1829–1842 (in Chinese with English abstract).

Landing, E.D., Geyer, G., Buchwaldt, R., and Bowring, S. A., 2015. Geochronology of the Cambrian: A precise Middle Cambrian U-Pb zircon date from the German margin of West Gondwana. Geological Magazine, 152(1): 28–40.

Liu, C.D., Mo, X.X., and Luo, Z.H., 2004. Mixing events between the Crust- and mantle-derived magmas in Eastern Kunlun: Evidence from zircon SHRIMP II chronology. Chinese Science Bulletin, 49(8): 828–834 (in Chinese with English abstract).

Li, X.H., Liu, X.M., and Liu, Y.S., 2015. Accuracy of LA-ICP-MS zircon U-Pb age determination: An inter-laboratory comparison. Science China (Earth sciences), 45(9): 1294–1303 (in Chinese with English abstract).

Luo, B.J., Zhang, H.F., Xiao, Z.Q., 2012. Petrogenesis and tectonic implication of the early Indosinian Meiwu Pluton in west Qinling, central China. Earth Science Frontiers, 19(3): 199–213 (in Chinese with English abstract).

Ludwig, K.R., 2008. User's Manual for Isoplot 3.7: A geochronological toolkit for Microsoft Excel. Berkeley Geochronology Centre Special Publication, 4: 70.

Mader, D., 1990. Palaeoecology of the Flora in Buntsandstein and Keuper in the Triassic of Middle Europe. New York: Gustav Fischer Verlag, 1–1582.

Mattinson, J.M., 2005. Zircon U-Pb chemical abrasion ("CA-TIMS") method: combined annealing and multi-step partial dissolution analysis for improved precision and accuracy of zircon ages. Chemical Geology, 220(1): 47–66.

Olsen, P.E.A., 1986. 40-million-year lake record of early Mesozoic orbital climatic forcing. Science, 234(4778): 842–848.

Qiu, X.W., Liu, C.Y., and Li, Y.H., 2009. Distribution characteristics and geological significances of tuff interlayers in Yanchang Formation of Ordos basin. Acta Sedmentologica sinica, 27(6): 1138–1146 (in Chinese with English abstract).

Retallack, G., 1975. The life and times of a Triassic lycopod. Alcheringa: An Australasian Journal of Palaeontology, 1(1): 3–29.

Roger, F., Malavieille, J., and Leloup, P.H., 2004. Timing of granite emplacement and cooling in the Songpan–Garzê Fold Belt (eastern Tibetan Plateau) with tectonic implications. Journal of Asian Earth Sciences, 22(5): 465–481.

Sun D., Feng Q., Liu Z., Lu C.J., and Xia L., 2017. Detrital zircon U-Pb of the Upper Triassic Yanchang Formation in

Southwestern Ordos basin and its provenance significance. Acta Geologica Sinica, 91(11): 2521–2544 (in Chinese with English abstract).
Wang, J.Q., Liu C.Y., Li, H., Wu, T.T., and Wu, J.L., 2017. Geochronology, Potential Source and Regional Implications of Tuff Intervals in Chang-7 Member of Yanchang Formation, South of Ordos Basin. Acta Sedmentologica sinica, 35(4): 691 –704 (in Chinese with English abstract).
Wang, Z.Q., and Wang, L.X., 1982. A new species of the Lycopsida Pleuromeia from the Early Triassic of Shanxi, China, and its ecology. Palaeontology, 25(1): 215–225.
Wang, D.Y., Xin, B.S., Yang, H., Fu J.H., Yao, J.L., and Zhang, Y., 2014. Zircon SHRIMP U-Pb age and geological implication of tuff at the bottom of Chang-7 member of Yanchang Formation in the Ordos basin. Science China (Earth science), 57(12): 2966–2977.
Wang, L.X., Xie, Z.X., and Wang, Z.Q., 1978. On the occurrence of pleuromeia from the qinshui basin in Shanxi province. Acta Palaeontologica Sinica, 17(2): 195–211 (in Chinese with English abstract).
Wang, Y.D., Jiang, D.X., and Xie, X.P., 2003. Late Triassic palynoflora and its environmental significance of tuweihe, Shanxi. Acta Sedimentologica Sinica, 21(3): 434–440 (in Chinese with English abstract).
Wotzlaw, J. F., Brack, P., and Storck, J. C., 2018. High-resolution stratigraphy and zircon U-Pb geochronology of the Middle Triassic Buchenstein Formation (Dolomites, northern Italy): precession-forcing of hemipelagic carbonate sedimentation and calibration of the Anisian–Ladinian boundary interval. Journal of the Geological Society, 175(1): 71–85.
Xie, X., 2007. Sedimentary record of Mesozoic intracontinental deformation in the south Ordos Basin, China (Ph.D. thesis). Laramie: University of Wyoming.
Yong, T.S., 1984. The discussion of the age of the yanchang group in erdos basin. Xinjiang Petroleum Geology, 1:58-60 (in Chinese with English abstract).
Yang, H., Zhang, W.Z., and Liu, X.Y., 2013. Key role of high-quality source rocks on the formation of low-permeability oil rich reservoirs in ordos basin. Journal of Earth Science and Environment, 35(04): 5–13 (in Chinese with English abstract).
Yin, H.F., Zhang, K.X., and Chen, N.S., 2013. People's Republic of China regional geological survey report (1:250000). Wuhan: China University of Geosciences Press, 1–457 (in Chinese with English abstract).
Yu, J.X., Huang, Q.S., Broutin, J., 2008. The early Triassic annalepis from western Guizhou and eastern yunnan, south china, Acta Palaeontologica Sinica, 47(3): 292–300 (in Chinese with English abstract).
Yu, J.X., Broutin, J., Huang, Q., and Grauvogel-Stamm, L., 2010. Annalepis, a pioneering lycopsid genus in the recovery of the Triassic land flora in South China. Comptes Rendus Palevol, 9: 479–486.
Zhao, M., H. Behr, H. Ahrendt, K. Wemmer, Z. Ren, and Z. Zhao, 1996. Thermal and tectonic history of the Ordos basin, China: Evidence from apatite fission track analysis, vitrinite reflectance, and K-Ar dating. AAPG Bulletin, 80: 1110–1134.
Zhang, W.Z., Yang, H., and Peng, P.G., 2009. Influence of volcanism on development of Chang 7 hydrocarbon source rock. Geochimica, 38(6): 573–582 (in Chinese with English abstract).
Zhang, Q.,Jiao, S.T., and Wu, H.R., 2013. The Chinese topographic map in Triassic. Journal of Palaeogeography, 15 (2): 181–202 (in Chinese with English abstract).
Zhang, H., Peng, P.A., and Zhang, W.Z., 2014. Zircon U-Pb ages and Hf isotope characterization and their geological significance of Chang 7 tuff of Yanchang Formation in Ordos basin. Acta Petrologica Sinica, 30(2): 565–575 (in Chinese with English abstract).
Zhou, D.W., Zhao, C.Y., and Li, Y.D., 1994. The geological Characteristic of Southwest Margin of Erdos Basin and its Relationship with the Qinling Mountain Belt. Beijing: Geological Publishing House, 1–178 (in Chinese with English abstract).

About the first author

ZHU Rukai, male, born in 1968 in Shaoxing City, Hunan Province; doctor; graduated from Peking University; Professorate senior engineer of Research Institute of Petroleum Exploration and Development. He is now interested in unconventional petroleum geology. Email: zrk@petrochina.com.cn; phone: 010-83598216.

About the corresponding author

CUI Jingwei, male, born in 1980 in Hengshui City, Hebei Province; doctor; graduate from China University of Petroleum, Beijing; Senior engineer of Research Institute of Petroleum Exploration and Development. He is now interested in unconventional petroleum geology and geochemistry. Email: cuijingwei@petrochina.com.cn; phone: 010-83595344.